Chapter 3

Immiscible Langmuir monolayers: Interactions between the polar head groups of cholesterol and octylcyanobiphenyl

3.1 Introduction

Mixed Langmuir monolayers are ideal systems to mimic biological membranes [1, 2]. Studies on mixed monolayers provide information about the interactions involved, miscibility and stability of the monolayer. It is known that cholesterol(Ch) is found in bilayer membranes and lipoproteins. Ch regulates the transport and barrier properties of the membranes [3]. Lung surfactant in the human body is composed of different kinds of lipids and proteins. This forms Langmuir monolayer at the alveolar air-water interface [4, 5, 6]. These mixed surfactants tend to reduce the surface tension to nearly zero. The mixed monolayer is required to be stable without going to the collapsed state during expiration. Lack or deficiency of these surfactants lead to respiratory distress syndrome(RDS) in the human body. Recent studies on mixtures of saturated lipid, unsaturated lipid with different concentration of cholesterol to mimic raft formation in membranes bring in some correlation between monolayer and unilamellar vesicles [7].

There are many reports on the mixed monolayer of cholesterol with biologically active lipids [8]. The mixed monolayer of cholesterol and oleic acid shows good miscibility [9]. This is attributed to Ch filling the voids in the bent shape molecule, oleic acid. With increase

in degree of unsaturation, it is observed that the miscibility behavior of Ch depends on the odd number or even number of double bonds. However, in both cases, the miscibility is good [10]. The mixed monolayer study of Ch with fatty acid like myristic acid reveals the miscibility in the expanded state and immiscibility in the condensed state [11]. It has been shown that Ch with a linear molecule like stearic acid is not miscible [12]. In a mixed monolayer of Ch with stearyl alcohol, which is also linear but with OH polar group, it is immiscible [13]. These studies indicate that the miscibility in the mixed monolayer mainly depends on the shape of the constituent molecules. Studies on the Ch and phospholipid mixed monolayer indicates a good miscibility [14, 15, 16]. These studies consider the interaction of the acyl chain with Ch rigid skeleton. It is found that the rigid hydrophobic skeleton of Ch stiffens the acyl chains of lipids [17]. The role played by the carbonyl oxygens(C=O) of phospholipid with the different positions of OH polar group in Ch and epi-cholesterol has also been addressed considering the hydrogen bond formation between them [18]. Though Ch and epi-cholesterol(epi-Ch) possess similar structures they differ in the absolute conformation of the hydroxyl group. This causes a difference in their interactions on membrane ordering, permeation to small ions and phase ordering [19]. Both Ch and epi-Ch causes condensation and ordering in membranes. But, the extent of ordering is less for epi-Ch when compared with Ch. For Ch, the 3β-OH group is found to be collinear and hence conducive for hydrogen bonding with carbonyl oxygens of phospholipid. The nature of hydrogen bonding in the mixed film for sphingomyelin and dipalmitoyl phosphatidyl choline has been studied [20]. These studies emphasis on the hydrogen bond donor-hydrogen bond acceptor type interactions between the polar groups. Recent simulations on aqueous cesium pentadecafluorooctanoate micellar systems indicate the slow reorientation of the interfacial water molecules [21]. The origin of this slow dynamics is attributed to the long-lived hydrogen bonds that an interfacial water molecule makes with the polar head group [22].

In most of these studies on mixed monolayers, the polar head is nearly in line with the rigid back bone of the molecules. The role of the polar head groups of different directionality and orientation in the mixed monolayer has not been probed.

In this chapter, we study the mixed monolayer behavior of cholesterol(Ch) with octylcyanobiphenyl(8CB) at the air-water interface to investigate the role of polar head groups and their interaction. It is known that both Ch and 8CB molecules are amphiphilic and form stable monolayer but their miscibility behavior has not been probed.

3.2 Experiment

Cholesterol was obtained from Aldrich and recrystallised using ethanol as a solvent. Octylcyanobiphenyl(Aldrich) was used as procured. The structure of cholesterol is shown in Figure 3.1. From this structure one can identify three parts. A planar and rigid steroid skeleton, a flexible isooctyl chain and a polar hydroxy group in 3β position. In cholesterol 96% of surface area is hydrophobic in nature [23]. The OH group in Ch can act as a hydrogen bond *donor* or *acceptor*.

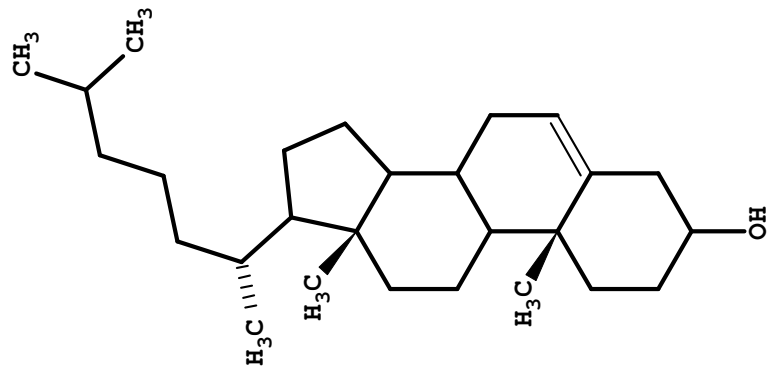

Figure 3.1: Structure of cholesterol(Ch)

Octylcyanobiphenyl(8CB) is a standard amphiphilic mesogenic molecule with a strong polar cyano head group having a dipole moment of 4 Db [24]. The structure of 8CB is shown

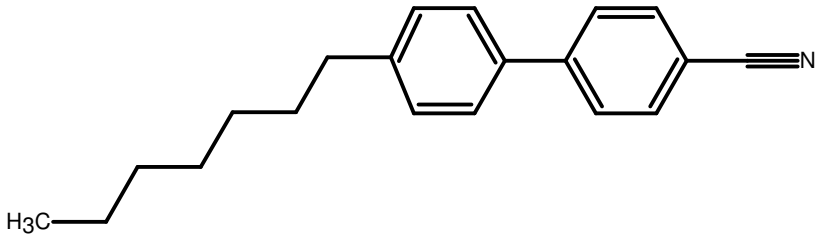

Figure 3.2: Structure of octylcyanobiphenyl(8CB)

in Figure 3.2. The hydrophilic C≡N group of 8CB can act as an hydrogen bond *acceptor*. The aromatic biphenyl can also form weaker hydrogen bonds.

The surface manometry experiments were carried out using NIMA 611M trough. The subphase used was ultra pure Millipore Milli-Q water(specific resistance > 18.2 MΩ-cm). The temperature(t) of the subphase was maintained at 22±0.5°C unless otherwise specified. The temperature of the trough was controlled by using a thermostat by circulating water. The relative humidity was about 85±5%. Stock solution of concentration 1.5 mM was prepared and used for making mixtures of required composition. The monolayer was spread using a microsyringe(Hamilton) and was equilibrated for 10 minutes to allow the solvent to evaporate. The sensitivity of the tensiometer was 0.1 mN/m. The monolayer was compressed at the rate of 0.02(Å^2/molecule)/second. Each π-A/M isotherm at a particular molefraction was repeated thrice. A moving point average of 20 points was used for these datas. This process of averaging helps to reduce the noise level in the data.

Epifluorescence microscopy was used to characterise the various phases indicated by the surface pressure(π) - area per molecule(A/M) isotherms. For these studies, a fluorescent dye 4-(hexadecylamino)- 7-nitrobenz-2 oxa-1,3 diazole(NBDHDA) obtained from Molecular Probes was used. Usually, about 0.5% molar concentration of the dye was added to the mixture. The monolayer doped with this dye was directly observed under a Leitz Metalux 3 microscope. The images were obtained using a photon intensified CCD camera(Model P46036A/V22, EEV) and was captured using a National Instruments(PCI-1411) frame grabber. A program written in LabView was used for capturing and storing the frames into bitmap format which was used for later analysis. The images were contrast enhanced equally for better clarity using GIMP software(GNU General Public Licensed). We have also carried out Brewster angle microscopy studies to characterize the phases.

3.3 Results

The π-A/M isotherms for the individual Ch and 8CB are shown in Figure 3.3. The Ch monolayer exhibits the phase sequence: gas(G), G + L_2, L_2, L_2 + 3D crystals. For Ch,

the detailed description of the π-A/M isotherm and microscopic studies were discussed in chapter-2. The π-A/M isotherm for 8CB exhibits the sequence of a coexisting G + L_1 phase,

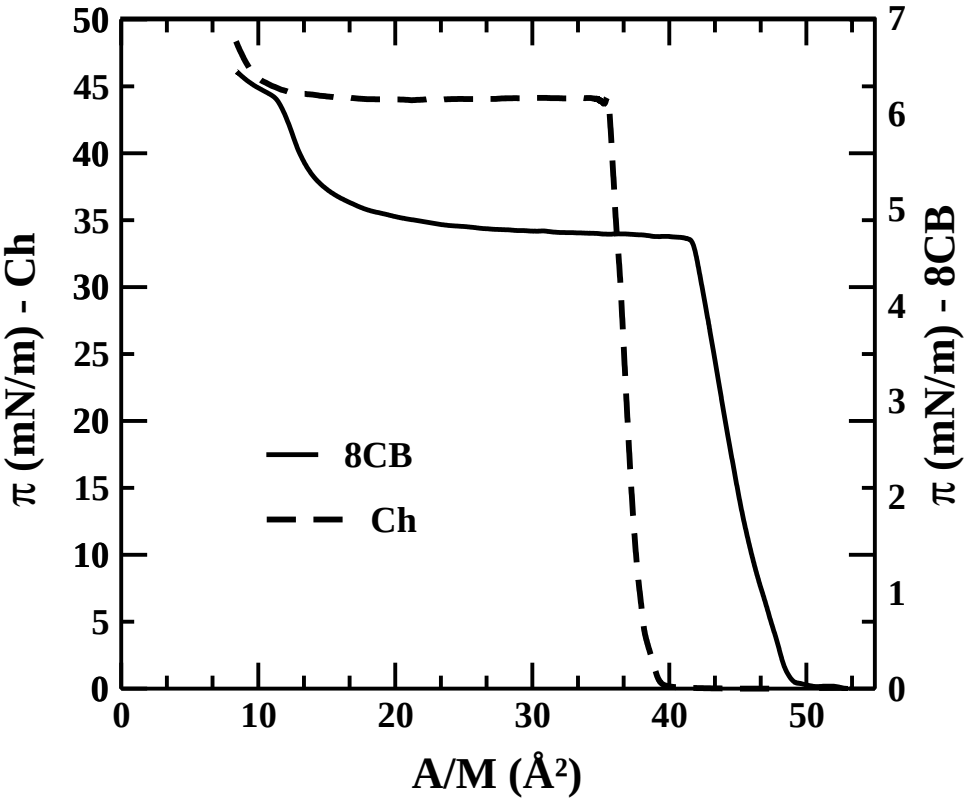

Figure 3.3: Surface pressure(π) - area per molecule(A/M) isotherm for individual cholesterol(Ch) and octylcyanobiphenyl(8CB) monolayer at t=22 °C. The vertical axis on the left gives the scale for Ch and the vertical axis on the right gives the scale for 8CB.

L_1 phase, coexisting L_1 + three layer(D_1) phase and a coexisting L_1 + D_1 + multilayer(D_2) phase. For 8CB, the limiting area, A_0(48 Å^2) is twice than that of a single benzene ring(24 Å^2) oriented normally at the A-W interface [25]. Hence, the monolayer of 8CB is loosely packed, and disordered at the A-W interface. The isotherms of Ch and 8CB are in good agreement with the reports in literature [25, 26, 27, 28, 29].

We have carried out the surface manometry experiments for Ch-8CB mixed monolayer at different compositions. This is shown in Figure 3.4. The plateau region of the π-A/M isotherm diminishes with increase in Ch mole fraction. The presence of a kink in the isotherm was observed above 0.6 MF of Ch in 8CB. The π-A/M isotherm shows the presence of two collapse pressures. The lower collapse pressure which is characteristic of 8CB is denoted

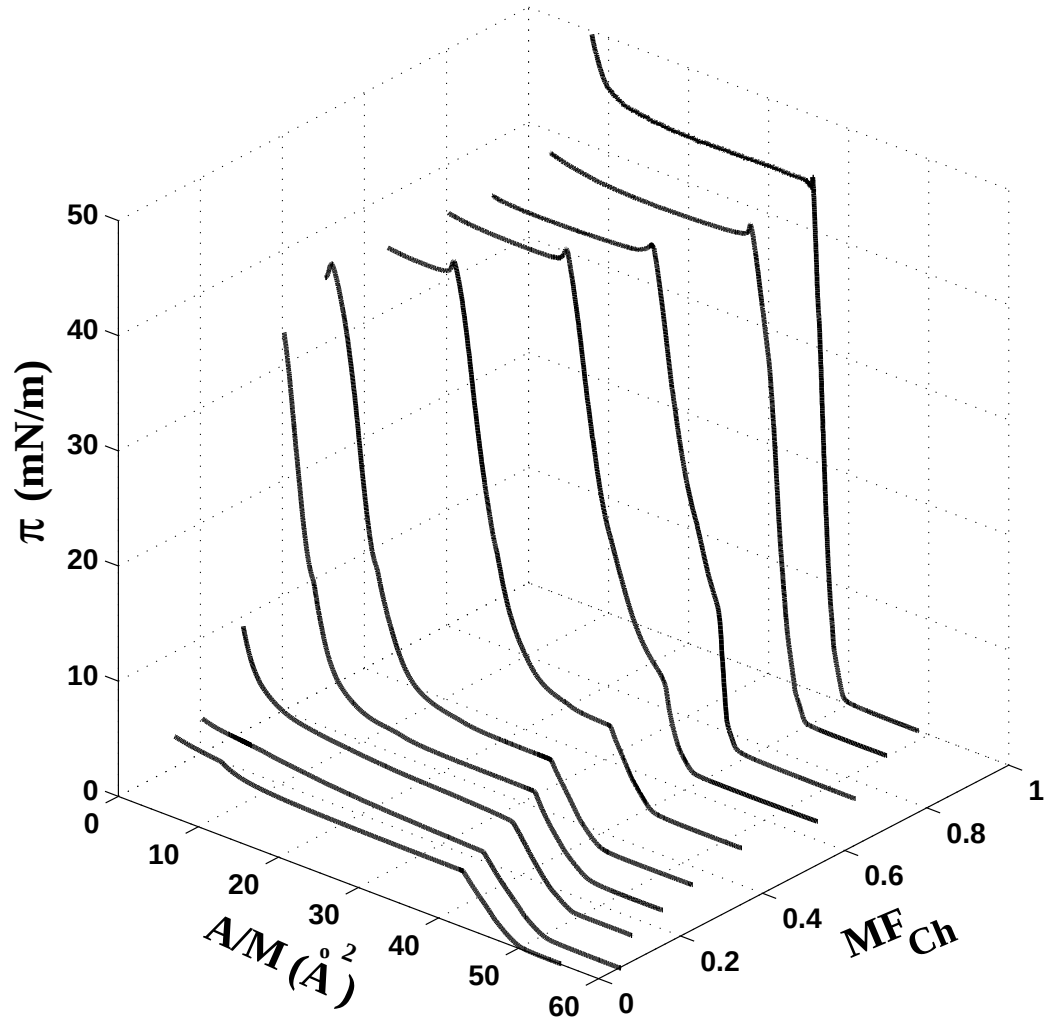

Figure 3.4: Surface pressure(π) - area per molecule(A/M) isotherm for Ch - 8CB mixed monolayer at different mole fraction(MF) of Ch in 8CB at t=22 °C.

by $\pi_{c(8CB)}$. The higher collapse pressure characteristic of Ch is denoted by $\pi_{c(Ch)}$. The collapse pressure variation with mole fraction of Ch is shown in Figure 3.5. The lower collapse pressure, $\pi_{c(8CB)}$, varies above 0.6 MF of Ch. The higher collapse pressure, $\pi_{c(Ch)}$ which is characteristic of Ch is independent of composition. To check the dependence of the collapse pressures and the isotherm behavior we have carried out our experiments at different temperatures and compositions of Ch. Figure 3.6 show the isotherms carried out for 0.5 MF and 0.9 MF of Ch in 8CB at different temperatures. The general trend in the isotherm behavior remains the same and there is not much difference in their collapse behavior. The epifluorescence images for cholesterol monolayer are described in detail in chapter-2. Our results are

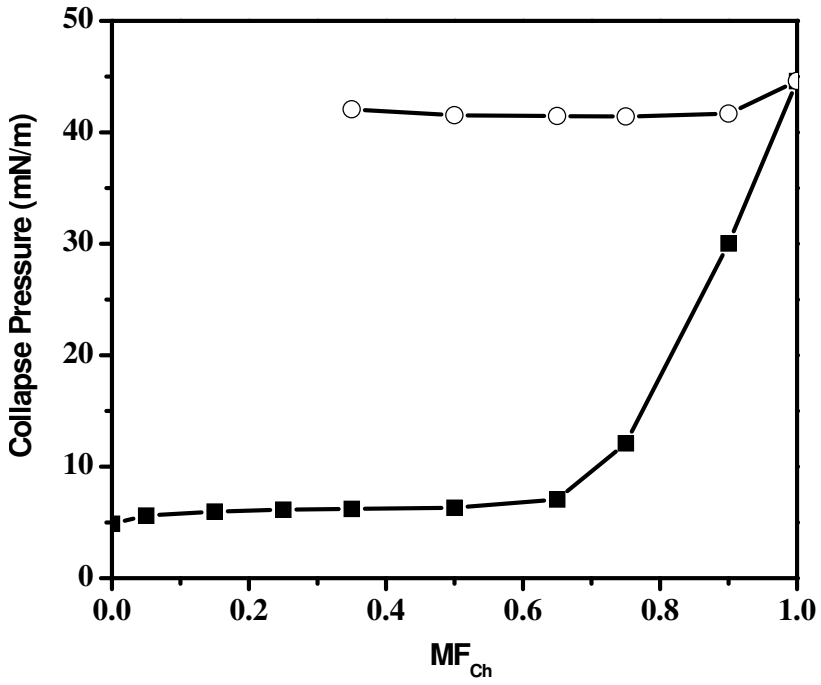

Figure 3.5: Variation of collapse pressure with increasing mole fraction(MF) of Ch in 8CB. The filled squares represent the lower collapse pressure, $\pi_{c(8CB)}$ and the open circles represent the higher collapse pressure, $\pi_{c(Ch)}$.

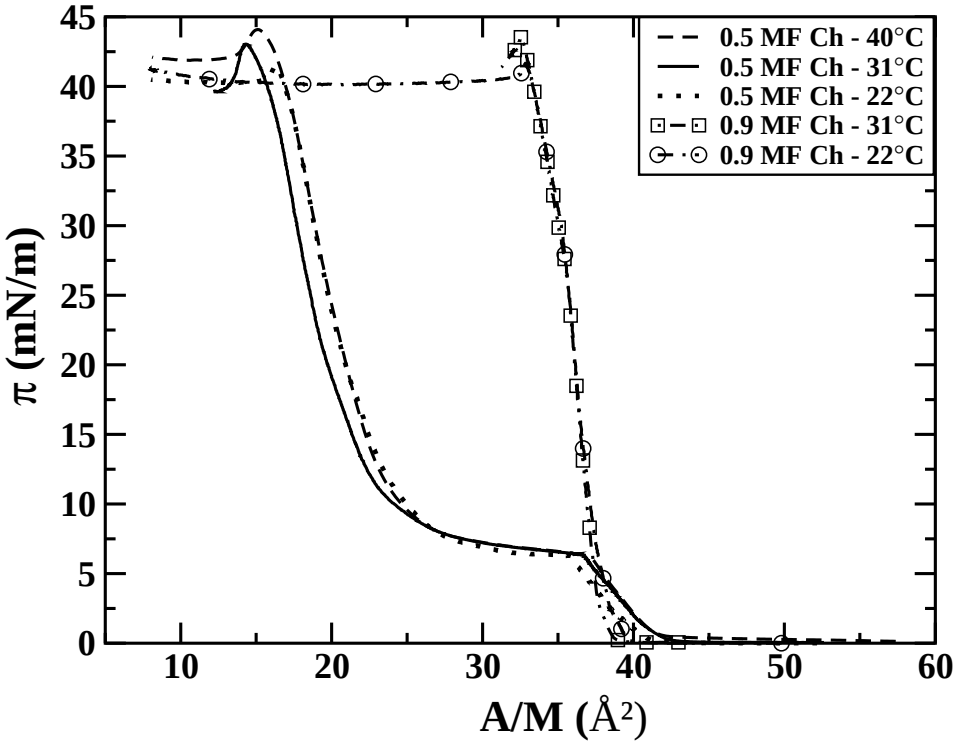

Figure 3.6: Surface pressure(π) - area per molecule(A/M) isotherms for Ch-8CB mixed monolayer at different compositions and temperatures.

in agreement with the epifluorescence [30] and Brewster angle microscopy [13] studies on Ch monolayer.

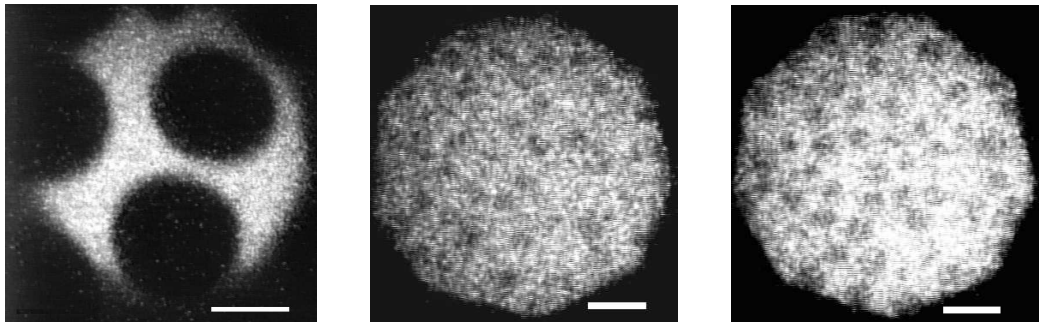

(a) 50.4 Å^2 (b) 30.5 Å^2 (c) 23.2 Å^2

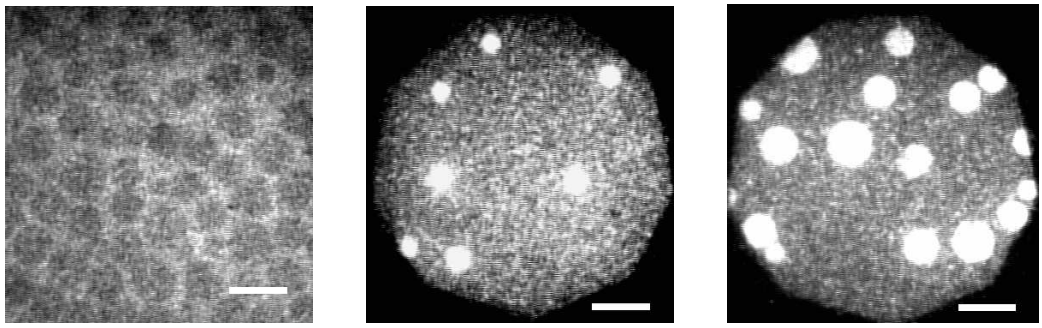

(d) 19.7 Å^2 (e) 11.0 Å^2 (f) 8.3 Å^2

Figure 3.7: Epifluorescence images for 8CB monolayer at A-W interface. Figure(a) shows the coexisting gas(dark) + L_1(background) phase. Figures (b) to (f) show the collapsed state. In Figures (b) to (d), the grey circular domains represent the trilayer(D_1) domains which coexist with L_1 phase. Figures (e) to (f) show the presence of still brighter multilayer domains(D_2) with D_1 phase in the background. Scale bar represents 50 μm.

The epifluorescence images for 8CB monolayer is shown in Figure 3.7. The sequence of images shows different coexisting phases with decreasing A/M. Figure 3.7(a) shows the foam like texture of Gas + L_1 domains. The gas domains appeared and the L_1 domain is bright. The fluorescence intensity of the L_1 phase of 8CB is relatively brighter than the L_2 phase of Ch for the same dopant concentration. Figures 3.7(b) to 3.7(d) show the nucleating circular bilayer over the monolayer. Here, this circular bilayer on top of a monolayer i.e., trilayer(D_1) domains appeared grey compared to the background L_1 phase. Figure 3.7(e) shows the bright, circular multilayer(D_2) domains nucleating from the uniformly covered background trilayer.

Figure 3.7(f) shows the increased presence of brighter multilayer domains. The background is the D_1 phase. The epifluorescence images for 0.25 MF of Ch in Ch-8CB mixed monolayer

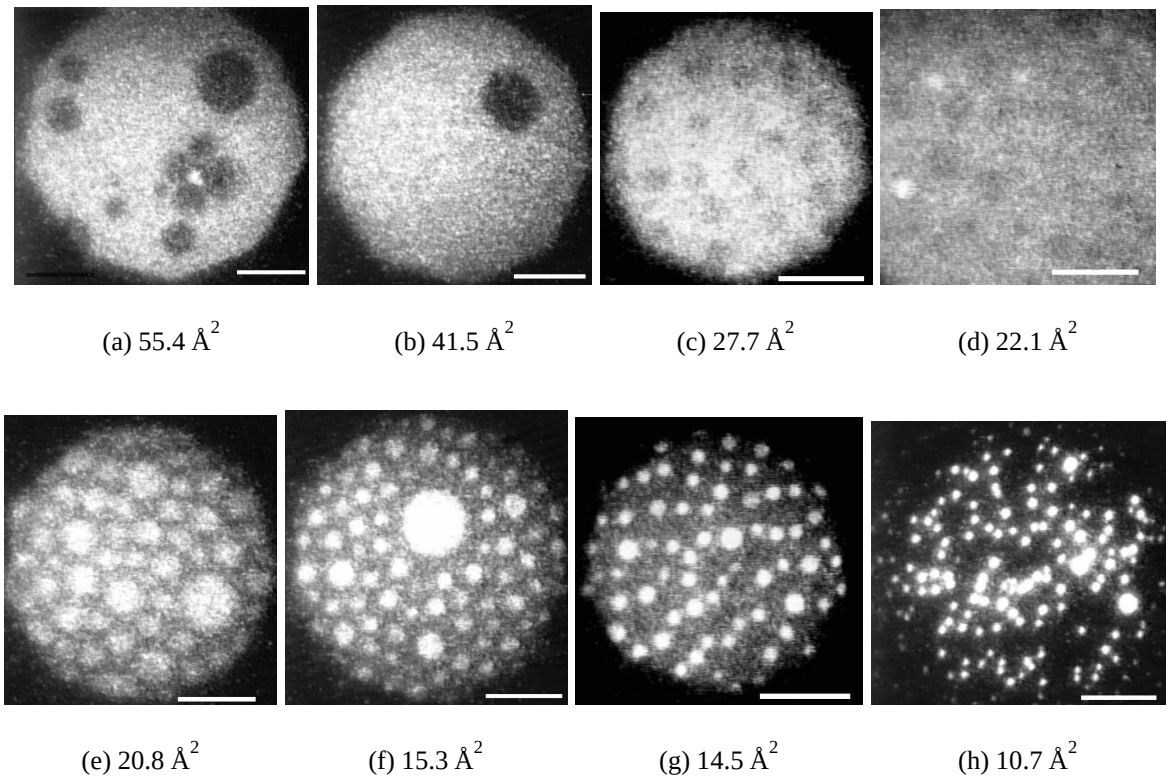

Figure 3.8: Epifluorescence images at 0.25 MF of Ch in Ch-8CB mixed monolayer at the A-W interface. In Figures (a) and (b), the coexisting G(dark) with predominantly present L_1 phase is seen. Figures (c) to (h) show the collapsed state. The faint grey circles are the trilayer(D_1) domains coexisting with L_1 + L_2 phase. Figures (e) to (g) show the still bright multilayer(D_2) domains nucleating from the D_1 domains and coexisting with L_2 phase. Figure(h) shows very bright D_2 domains coexisting with Ch crystallites. Scale bar represents 50 μm.

is shown in Figure 3.8. Figures 3.8(a) and 3.8(b) shows the presence of Gas domains with L_1 and L_2 phase. In Figure 3.8(c) circular bilayer(dark) on top of monolayer(D_1 phase) is seen to nucleate from the background L_1 phase. Figures 3.8(d) and 3.8(e) show the nucleation of multilayer domains from the uniformly covered D_1 domains. Figures 3.8(f) and 3.8(g) shows the increased number of brighter multilayer D_2 domains. Figure 3.8(g) shows the D_2 domains coexisting with crystallites of Ch. The epifluorescence images for 0.5 MF of Ch in Ch - 8CB system are shown in Figure 3.9. The presence of two different fluorescent intensity domains are seen in Figure 3.9(a)(top right corner) and Figure 3.9(b)(top region). The

brighter domain is L_1 phase which is 8CB rich. The less brighter domain is L_2 phase. The gas phase is in the background. Figure 3.9(c) shows the predominantly present L_2 phase with L_1 phase coexistence. In Figure 3.9(d), the trilayer D_1 domains are seen to nucleate from the L_1 phase. The L_2 phase is in the background. Figure 3.9(e) shows the presence of brighter D_2 domains with L_2 phase in background. Figure 3.9(f) shows the presence of D_2 domains with the bulk Ch crystallites in the background. The epifluorescence images for 0.75 MF of Ch

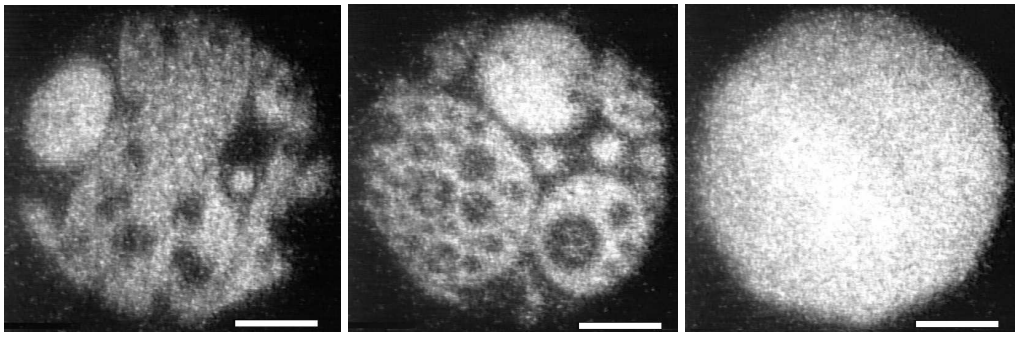

(a) 60.9 Å^2 (b) 49.8 Å^2 (c) 39.7 Å^2

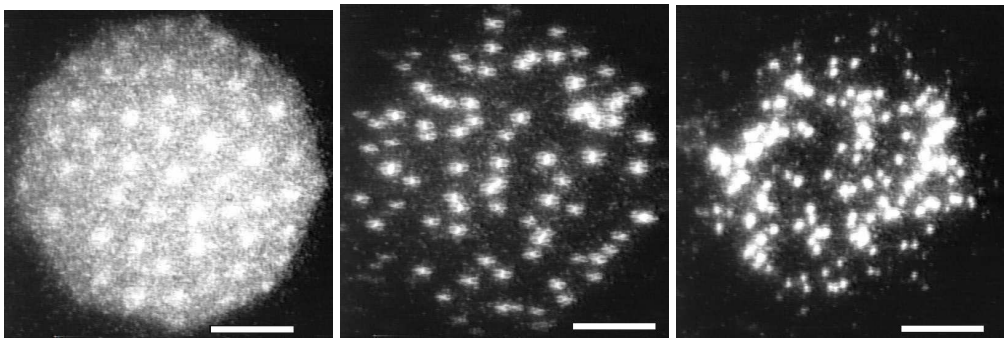

(d) 30.4 Å^2 (e) 21.9 Å^2 (f) 9.7 Å^2

Figure 3.9: Epifluorescence images at 0.5 MF of Ch in Ch-8CB mixed monolayer at the A-W interface. In Figures (a) and (b), $G + L_1 + L_2$ coexistence phases are clearly seen. Here the brighter domains(top left corner in (a) and top region in (b)) represent 8CB rich L_1 phase. The other less bright domains represent Ch rich L_2 phase. The dark region represents the gas phase. Figure(c) shows the predominant L_1 phase coexisting with L_2 phase. Figure(d) shows the presence of bright D_1 domains in the L_2 phase background. Figure(e) shows the coexistence of $L_2 + D_2$ phase. Here the D_2 domains are much brighter and in contrast the L_2 phase in the background appeared dark. Figure(f) shows the collapsed state of Ch crystallites(dark background) coexisting with D_2 phase. Scale bar represents 50 μm.

in Ch-8CB mixed monolayer is shown in Figure 3.10. The immiscible monolayer phases L_1

and L_2 are clearly visible in Figures 3.10(a) and 3.10(b). The brighter phase is L_1 phase, the less brighter phase is L_2 phase and the gas phase appeared . Figure 3.10(c) shows bright L_1 domains coexisting with L_2(background) phase. The L_1 phase directly transformed to much brighter multilayer(D_2) domains without going via a three layer D_1 phase. This is shown in Figures 3.10(d) and 3.10(e). The collapsed crystallites of Ch are seen with coexisting multilayer(D_2) (Figures 3.10(f) to 3.10(h)). This direct transformation from L_1 to D_2 phase is reflected as a kink in the isotherm at the lower collapse pressure. The Ch crystallites nucleate above the second collapse pressure. To analyse the nature of the collapse and to rule out

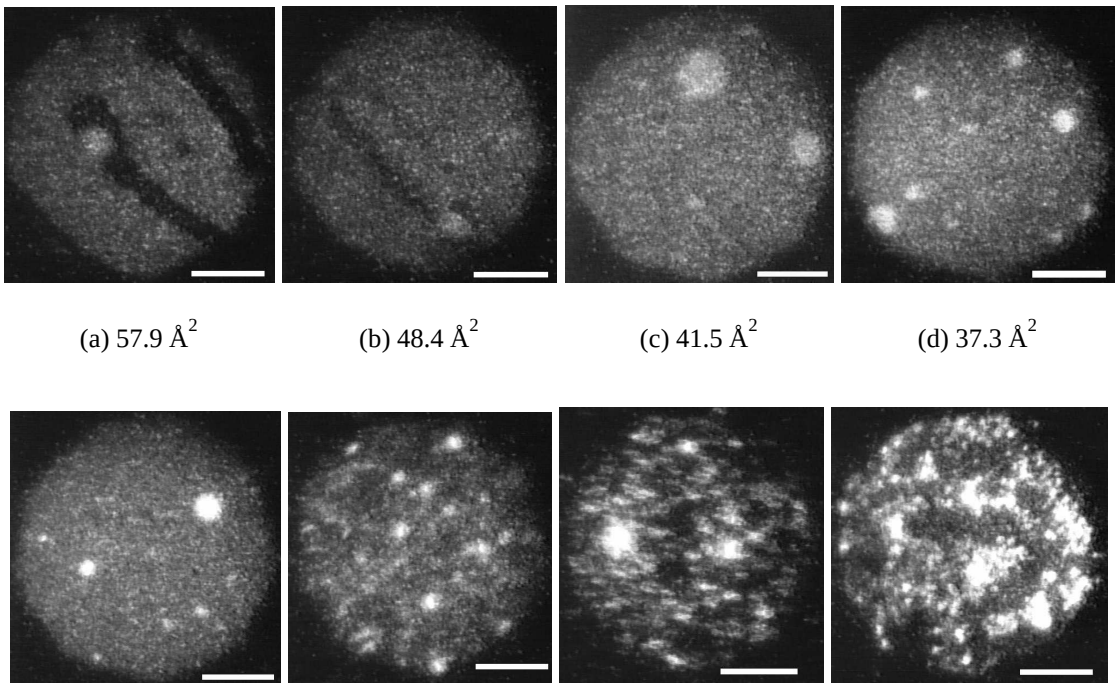

(a) 57.9 Å^2 (b) 48.4 Å^2 (c) 41.5 Å^2 (d) 37.3 Å^2

(e) 35.9 Å^2 (f) 33.6 Å^2 (g) 27.7 Å^2 (h) 10.0 Å^2

Figure 3.10: Epifluorescence images at 0.75 MF of Ch in Ch-8CB mixed monolayer at the A-W interface. Figure(a) shows the $G + L_1 + L_2$ coexistence phase. Here the stripes represent the gas phase, the single brighter domain is the L_1 phase, and the background is the L_2 phase. Figures (b) and (c) show the bright L_1 domains and the background L_2 in coexistence. Figures (d) and (e) represent the coexistence of L_2(background) and D_2 domains(very bright). Figures (f) to (h) show the D_2 domains(very bright) coexisting with crystallites of Ch(dark background) in the collapsed state. Scale bar represents 50 μm.

the artifacts due to the fluorescent dye we have carried out Brewster angle microscopy for Ch-8CB mixed monolayer at different compositions. Figure 3.11 shows the collapsed state

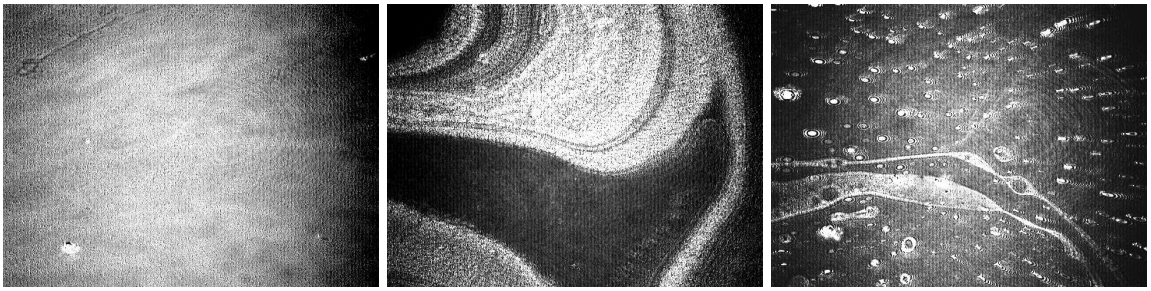

(a) 28.5 Å^2 (b) 33.2 Å^2 (c) 33.2 Å^2

Figure 3.11: Brewster angle microscopy images for Ch-8CB mixed monolayer at different mole fractions above the lower collapse pressure, $\pi_{c(8cb)}$. Figure(a) represents the collapsed state at 0.25 MF of Ch in 8CB. The small bright dots are the trilayers(D_1) coexisting with the L_1 + L_2 phase in the background. Figure(b) represents the collapsed state at 0.5 MF of Ch in 8CB. The small bright dots are the multilayers(D_2) coexisting with L_1 + L_2 phases(background). Figure(c) represents the collapsed state at 0.75 MF of Ch in 8CB. The small bright dots are the multilayer domains which coexist with L_2 phase in the background. Scale of each image is 6.4 x 4.8 mm^2.

above the lower collapse pressure($\pi_{c(8CB)}$) at 0.25, 0.5 and 0.75 MF of Ch in 8CB. We have constructed the phase diagram for Ch-8CB mixed monolayer based on our surface manometry, epifluorescence and BAM studies. This is shown in Figure 3.12. The occurrence of different monolayer and multilayer phases are depicted with varying mole fraction of Ch in 8CB. The coexistence of L_1 and L_2 separated phases are seen in the MF range 0.1 MF to 0.9 of Ch in 8CB. The occurrence of three layer D_1 and multilayer(D_2) phases are seen to nucleate from the background L_1 phase indicating that the L_1 is 8CB rich. The crystallites are seen to grow from the L_2 phase indicating that it is Ch rich.

3.4 Discussions

We have chosen a system of Ch with almost saturated core and 8CB with an aromatic core. The interactions between them are weak. It has been reported that in a monolayer with biphenyl or terphenyl derivative when the phenyl ring is replaced by cyclohexane or bicyclooctane, the stability of the monolayer is reduced considerably [31]. In these molecules, the C≡N polar group is retained and the hydrophobic part was changed with more bulky and sat-

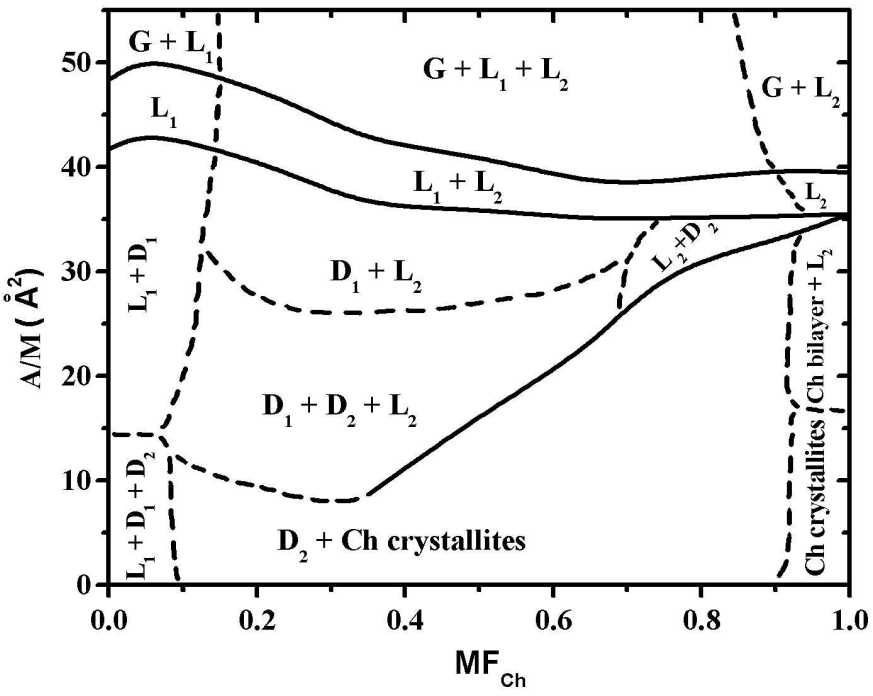

Figure 3.12: Phase diagram of Ch-8CB mixed monolayers at t=22 °C. Here, the continuous lines indicate the actual phase boundaries and the dashed lines indicate the approximate phase boundaries.

urated cores which suppresses the formation of smectic LC phases. Hence, we did not take the hydrophobic contributions into account as its interactions are minimal. Our studies using surface manometry and epifluorescence microscopy at different compositions indicated that the mixed monolayers were immiscible. We find from the isotherm two collapse pressures in which the higher collapse pressure did not change with composition and the lower collapse pressure changed above 0.6 MF of Ch. This indicated that the interactions are weak between the molecules in the mixed monolayer. For an ideal mixed monolayer, the collapse pressure should vary linearly with composition. If a mixed monolayer exhibits two collapse pressures which are independent of composition, then they are said to be immiscible [1]. The epifluorescence images at 0.25 MF, 0.5 MF and 0.75 MF of Ch in 8CB indicated the presence of two monolayer phases whose fluorescent intensities were different. The solubility of the fluorescent dye in 8CB rich L_1 phase was more. Hence it appeared brighter in

appearance than when compared with Ch rich L_2 phase. Hydrogen bonding interactions are important in understanding their role in proteins and lipids in biological systems. Numerous experiments and simulations were done and it is still of continuing interest. The presence of a hydrophobic solute changes the hydrogen bonded network. This is of entropic origin since the hydrogen bond configurations changes in water.

The surface hydrogen bond networks are important since it decides the interfacial properties like surface tension and interfacial viscosity of water and it is still a topic of research interest. Spectroscopy techniques are powerful tools to reveal the dynamics of these hydrogen bonds at the interface. Shen and his co-workers carried out sum frequency generation(SFG) experiments [32] on vapour-water interface. Their results indicated that greater than 20% of the surface molecules were polar oriented with a free non-hydrogen-bonded O-H bond pointing towards air and tilted about 38°. The presence of a monolayer like stearyl alcohol leads to ordered structure at the interface. The presence of OH polar group in stearyl alcohol exhaust these free dangling OH bonds. Thus the polar group of amphiphilic molecule enhances the surface ordering due to the formation of new hydrogen bonds with the water. The water molecule can form hydrogen bonds with C≡N group of 8CB. The hydrogen bonding nature of CN bond itself has not been investigated in great detail [33]. The different possibilities of hydrogen bonding in CN are shown in Figure 3.13. The interfacial water structure

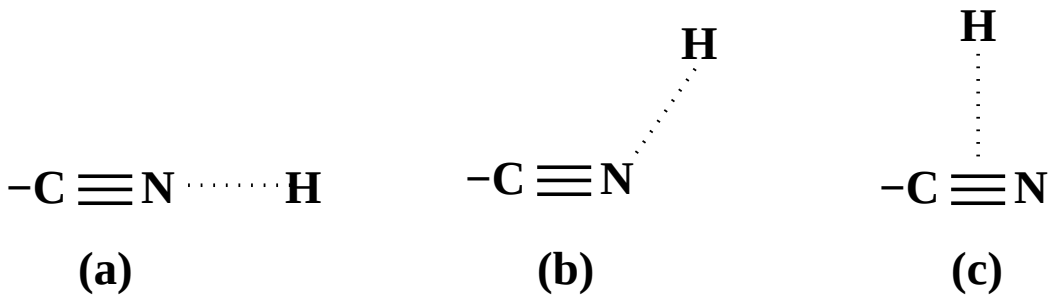

Figure 3.13: Possible hydrogen bondings with CN group: (a) Hydrogen bonds with Nitrogen group, (b) Intermediate bonding and (c) Bonding with π electron cloud.

is known to be quite different from that of bulk due to the presence of broken bonds at the interface. Typical time scale for a bond to break and form is in the pico second regime. The hydrogen bonds formed in water are highly specific and directional. The presence of polar

groups like -OH and -C≡N can affect this hydrogen bonded network to a large extent [34]. The presence of polar OH group in cholesterol which is normal and in line with the rigid skeleton of Ch can form hydrogen bonds with water and develop a network. The importance of donor and acceptor hydrogen bonding directionality has been discussed in great detail [33]. This hydrogen bonded network and the directionality due to OH of Ch may be different from the hydrogen bonded network caused by the presence of strongly polar C≡N of 8CB which is tilted from the normal by about 60° [25]. The strong C≡N dipole can polarize the environment and can reconfigure the network. Shen et.al., [35] using second harmonic generation technique have probed the orientation of polar molecules on rigid polar substrates like polyimide and quartz. They have also carried out experiments on nCB at air-water interface whose surface is penetrable. Their experimental results for the case of polar rigid substrates indicate that the tilt angle of nCB varies from 72°-82° with alkyl chain length ranging from 1-12. For nCB, at the A-W interface, the tilt angle is found to be independent of alkyl chain length. This was explained by considering the hydrogen bonding interactions which might also reorient the water molecules. The energy required for placing a C≡N, a CH in the biphenyl ring and a CH_2 into bulk water are of the order -20k_bT, 1.2 k_bT and 2.0k_bT respectively [36].

From these results and from our experiments, we suggest that this orientational differences between the polar head groups in their hydrogen bonding nature, OH in Ch and C≡N in 8CB have resulted in this observed immiscibility. Schematically, this is depicted in Figure 3.14. Here the bound water molecules attached to the polar groups of Ch and 8CB are oriented locally in different directions due to the normal orientation of Ch and tilted orientation of 8CB. The absence of correlation between the local orientational order may result in the observed immiscible behavior for the Ch-8CB mixed monolayer.

There are reports on the miscibility nature in the mixed monolayer of cholesterol and stigmastanil phosporylcholine(SPC) [37]. SPC also possess the same hydrophobic rigid skeleton of Ch as that of Ch. These hydrophobic skeletons are oriented normal at the A-W interface. However, the hydrophilic polar groups are different and are oriented at an angle. Their

surface manometry experiments indicate a better miscibility at different temperatures. The increase in the limiting area per molecule(A_0) of the SPC monolayer was due to the electrostatic repulsion between the dipoles. The observed miscibility was attributed to the *dielectric* action of Ch which decreases the electrostatic repulsions between SPC molecules. The ob-

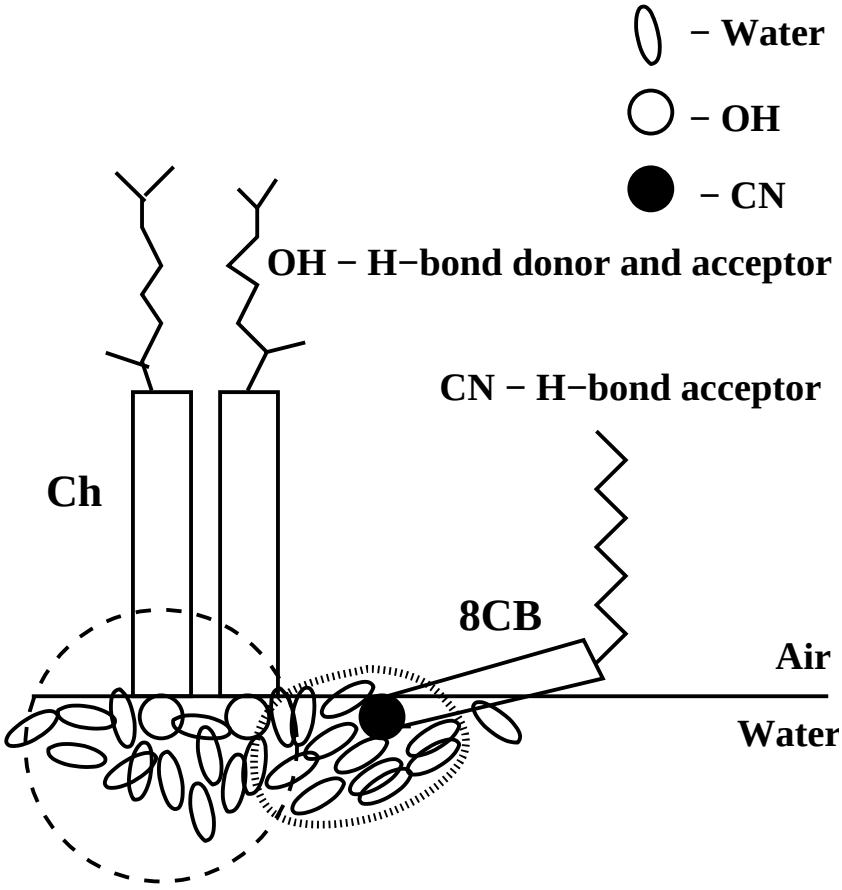

Figure 3.14: Schematic arrangement of cholesterol(Ch) and octylcyanobiphenyl(8CB) molecules in the mixed monolayer at the A-W interface. Here, the orientational differences in terms of hydrogen bonding between the polar groups is shown. Like molecules interaction are preferred resulting in immiscibility.

served immiscibility in Ch-8CB mixed monolayer can be explained using Crisp's phase rule [38]. According to this phase rule, the degrees of freedom(F) for the mixed monolayer at constant temperature and external pressure is,

$$F = C_b + C_s - P_b - q + 1 \tag{3.1}$$

where, C_b is the number of components in the bulk, C_s is the number of components at the surface, P_b is the bulk phase and q is the monolayer phase. In our case, C_b=2(air and water).

C_s=2(Ch and 8CB), P_b=3(gas, liquid and D_1) and q=2(L_1 and L_2)monolayer phases. Then from equation(3.1), F=0. This indicates that the collapse pressure is independent of the composition in the mixed monolayer and is in agreement with our results upto 0.6 MF of Ch. The change in the collapse pressure above 0.6 MF is due to the transformation of L_1 to D_2 domains. Hence, the Ch-8CB monolayer phase separates in the MF range of 0.15 to 0.9 of Ch. The component of the monolayer, which had low value of collapse pressure($\pi_{c(8CB)}$), gets squeezed out of the mixed monolayer.

Our study on Ch-8CB mixed monolayer indicated a phase separation in the range 0.15 to 0.9 MF of Ch in 8CB. This conclusion is based on our surface manometry, epifluorescence and Brewster angle microscopy techniques. Our results are in accordance with the Crisp's phase rule for mixed monolayer systems. We attribute this observed immiscibility to the orientational and directional differences of the hydrogen bonding of the polar head groups with water molecules. In the next chapter, we present our studies on the mixed monolayer with a molecule possessing a weakly polar group and a strongly polar group retaining the same hydrophobic groups.

Bibliography

[1] G.L. Gaines Jr., *Insoluble monolayers at air-water interface*, Wiley-Interscience, 1966.

[2] K.S. Birdi, *Lipid and biopolymer monolayers at liquid interfaces*, Plenum:NY, 1989.

[3] K. Simons and E. Ikonen, Science, **290**, 1721, 2000.

[4] J. Johansson and T. Curstedt, Eur. Jour. Biochem., **244**, 675, 1997.

[5] U. Pison, R. Herold and S. Schurch, Coll. Surface, **114**, 165, 1996.

[6] K.Y.C. Lee, A. Gopal, A. Nahmen, J.A. Zasadzinski, J. Majewski, G.S. Smith, P.B. Howes and K. Kjaer, Jour. Chem. Phys., **116**, 774, 2002.

[7] S.L. Veatch and S.L. Keller, Phys. Rev. Lett., **89**, 268101, 2002.

[8] L. Finegold, *Cholesterol in membrane models*, CRC Press:Boca Raton - FL, 1993.

[9] Y.K. Rao and D.O. Shah, Jour. of Coll. Int. Sci., **137**, 25, 1990.

[10] R. Seoane, P. Dynarowicz-tstka, J. Minones Jr and I. Rey-Gomez-Serranillos, Coll. Poly. Sci., **279**, 562, 2001.

[11] K. Motomura, T. Terazono, H. Matuo and R. Matuura, Jour. of Coll. Int. Sci., **57**, 52, 1976.

[12] C.E. McNamee, G.T. Barnes, I.R. Peng, J.H. Steitz and R. Probert, Jour. of Coll. Int. Sci., **207**, 258, 1998.

[13] R. Seoane, J. Minones, O. Conde, J. Minones Jr., M. Casas and E. Iribarnegaray, J. Phys. Chem. B, **104**, 7735, 2000.

[14] D. Chapman, N.F. Owens, M.C. Philip and D.A. Walker, Biochim. Biophys. Acta, **183**, 458, 1969.

[15] P. Mattjus, R. Bittman and J.P. Slotte, Langmuir, **12**, 1284, 1996.

[16] L.D. Worthman, K. Nag, P.J. Davis and K.M.W Keough, Biophys. Jour., **72**, 2569, 1997.

[17] M. Sugahara, M. Uragami, X. Yan and S.L. Regen, J. Am. Chem. Soc., **123**, 7939, 2001.

[18] C. Huang, Nature, **259**, 242, 1976.

[19] T. Rog and M. Pasenkiewicz-Gieurula, Biophys. Jour., **84**, 1818, 2003.

[20] E. Mombelli, R. Morris, W. Taylor and F. Fraternalli, Biophys. Jour., **84**, 1507, 2003.

[21] S. Balasubramanian and B. Bagchi, Jour. Phys. Chem. B, **106**, 3668, 2002.

[22] S. Balasubramanian, S. Pal and B. Bagchi, Phys. Rev. Lett., **89**, 115505, 2002.

[23] R. Johann, C.Symietz, D. Vollhardt, G. Brezesinski and H. Mohwald, J. Phys. Chem. B, **104**, 8512, 2000.

[24] D.A. Dunmur, M.R. Manterfield, W.H. Miller and J.K. Dunleavy, Mol. Cryst. Liq. Cryst., **45**, 127, 1978.

[25] J. Xue, C.S. Jung and M.W. Kim, Phys. Rev. Lett., **69**, 474, 1992.

[26] H. Rapaport, I. Kuzmenko, H. Berfeld, K. Kjaer, J. Als-Nielsen, R. Popovitz-Biro, I. Weissbuch, M. Lahav and L. Leiserowitz J. Phys. Chem. B, **104**, 1399, 2000.

[27] N.G.M.D. Mul and J.A. Mann Jr., Langmuir, **10**, 2311, 1994.

[28] M.C. Friedenberg, G.G. Fuller, C.W. Frank and C.R. Robertson, Langmuir, **10**, 1251, 1994.

[29] K. A. Suresh and A. Bhattacharyya, Langmuir, **13**, 1377, 1997.

[30] J.P. Slotte and P. Mattjus, Biochim. Biophy. Acta, **1254**, 22, 1995.

[31] M.F. Daniel, O.C. Lettington and S.M. Small, Thin Solid Films, **99**, 61, 1983.

[32] Q. Du, R. Superfine, E. Freysz and Y.R. Shen, Phys. Rev. Lett., **70**, 2313, 1993.

[33] G.R. Desiraju and T. Steiner, *The weak hydrogen bond : In structural chemistry and biology*, Oxford Science Publications, 1999.

[34] D. Chandler, Nature, **417**, 491, 2002.

[35] X. Zhuang, D. Wilk, L. Marrucci and Y.R. Shen, Phys. Rev. Lett., **75**, 2144, 1995.

[36] J.N. Israelachvilli, *Intermolecular and Surfaces Forces*, Academic:London, 1985.

[37] R. Seoane, J. Minones, O. Conde and J. Minones Jr., Coll. and Surf. A: Physicochem. Eng. Aspects, **174**, 329, 2000.

[38] D.J. Crisp, *Surface Chemistry Suppl. Research*, Butterworths:London, 1949.